Triple-channel terahertz filter based on mode coupling of cavities resonance system

JiaMing Xu, Lin Chen, XiaoFei Zang, Bin Cai, Yan Peng et al.

Citation: Appl. Phys. Lett. **103**, 161116 (2013); doi: 10.1063/1.4826456
View online: http://dx.doi.org/10.1063/1.4826456
View Table of Contents: http://apl.aip.org/resource/1/APPLAB/v103/i16
Published by the AIP Publishing LLC.

Triple-channel terahertz filter based on mode coupling of cavities resonance system

JiaMing Xu, Lin Chen,[a] XiaoFei Zang, Bin Cai, Yan Peng, and YiMing Zhu[a]
Engineering Research Center of Optical Instrument and System, Ministry of Education and Shanghai Key Lab of Modern Optical System, University of shanghai for Science and Technology, Shanghai 200093, China

(Received 24 June 2013; accepted 30 September 2013; published online 17 October 2013)

A high-quality triple-channel terahertz filter based on silicon multi-cavity resonant system has been experimentally investigated by using backward wave oscillator. Theoretical methods have been employed to analyze physical origin of the resonances and the transmission properties. We find that the lower transmission peak comes from the Fabry-Perot resonance in the side two thick cavities and the two higher peaks are caused by the symmetrically and asymmetrically coupling of the two thin cavities in the middle. The resonant peaks show blue shift by increasing the incident angle, which are attributed to the change of effective refractive indices. © *2013 AIP Publishing LLC*. [http://dx.doi.org/10.1063/1.4826456]

In recent years, with the development of terahertz (THz) technology, many potential applications such as biotechnology, THz communications, medical imaging, and plasma diagnostics have been realized.[1–6] In these applications, it is vital and necessary to manufacture high quality factor (HQ) THz filter. There are many methods such as grating,[4] surface plasmon polaritons,[5] and quantum well[6] can be utilized to fabricate HQ THz filters. Recently, the filter based on one-dimension (1-D) photonic crystals (PCs)[7] with one defect has been widely studied due to their HQ feature, simple configuration, and low cost. However, the Fabry-Perot resonance (FPR)[8] among large number of lossy silicon wafers reduces the maximum transmissivities of the filters based on PCs.[7] On the contrary, THz multi-cavity resonant system with the small number of periods has the advantages of multiple channels and high transmissivities, which makes this type of structure be potential device to realize the THz wavelength division multiplexing (THz-WDM).[9] However, the interaction of more than two cavities (especially two cavities with different thickness) and its physical origin in formation of transmission have few been reported. In this paper, we design, simulate, and analyze a multi-cavity resonant system which has three HQ transmission peaks. We use results from both calculation and simulation to analyze the mechanism in the formation of all three peaks observed in the experiment. We indicate the interactions exist between any adjacent two cavities. Besides, the influences of different incident angles on three resonant frequencies are also discussed.

The aim of our study is to find a low-cost and easily fabricated filter with good transmission properties. Considering the fact that the more difference of two material's permittivities (ε) is, the stronger the FPR effect is, we choose silicon ($\varepsilon = 11.87\text{-}0.006i$, i is the imaginary unit) and air ($\varepsilon = 1$) to fabricate our sample. The transfer matrix method (TMM) has been used to design sample as calculation method.[10–16]

First, as more silicon wafers will descend the transmissivity of the sample significantly, the designed structure consists of as few silicon wafers as possible. We use "S" stands for silicon, "A" and "R" stand for the thick and thin air layer. The simplest configuration as SAS cannot generate the HQ transmission peak, whose full width at half maximum (FWHM) is too large to use as a feasible device. The systems which consist of two cavities such as SASAS can only form two transmission peaks (red line in Fig. 1). Similarly, the systems such as SASASAS and SASRSAS cannot reach our aim. The transmission curve of SASASAS is like the one of SASAS expect the peaks are narrower and have higher quality factor. The two lower peaks of the transmission curve of SASRSAS are too close to be distinguished them, which is depended on the far distance of the coupling cavities (green line in Fig. 1). Thus, to reach our aim, we use SASRSRSAS structure as our device in the experiment.

We consider the thicknesses of silicon wafers as constants and adjust the thicknesses of air layers to optimize the

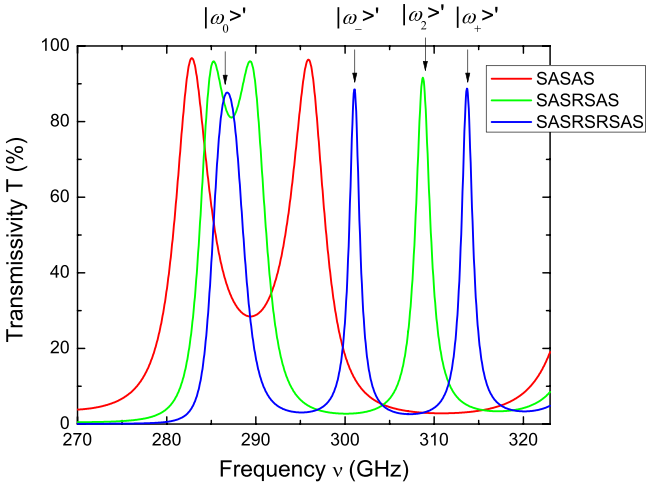

FIG. 1. Transmission curves of different configuration at normal incidence obtained by TMM.

[a]Authors to whom correspondence should be addressed. Electronic addresses: linchen@usst.edu.cn and ymzhu@usst.edu.cn

transmission properties of our filter. In the optimization, we use the following evaluation function:

$$F = [\mathrm{corr}(\nu_0) + \min(T_{\max})] \times 100 + \min(Q), \quad F \to \max, \tag{1}$$

where ν_0, $T_{\max}$, and Q are the central frequencies, the maximum transmissivities, and the quality factors of the three transmission peaks, respectively. The quality factor is defined as the ratio of the central frequency to FWHM. Besides, the corr(ν_0) is the linear correlation coefficient of three central frequencies and min($T_{\max}$), min(Q) stand for the minimum value of three peaks. This expression can ensure all of three peaks with equal distances, high maximum transmissivities, and HQ. A part of calculated results is listed in Table I. Due to its largest value, the combination (A, R) = (1.04, 0.94) mm was chosen as the optimal thicknesses in the experiment.

The sample we fabricated consists of five $\sim 3 \times 3\,\mathrm{cm}^2$ square pieces of silicon cut from single Si wafer with high resistance and four stainless spacers of different thicknesses (shown in Fig. 2(a)). The sheet resistance, crystal orientation, thickness, and diameter of wafer are $20000 \sim 28000\,\Omega$, $\langle 100 \rangle \pm 0.5°$, $525 \pm 15\,\mu$m, and 100 ± 0.3 mm, respectively. The four stainless spacers are used: Two are 1.04 mm-thick and others are 0.94 mm-thick. A metal clip is used to sandwich the pieces and spacer of the multi-cavity resonant structure. As shown in Fig. 2(b), we also used two 0.5 mm-thick spacer to distribute the pressure of the clip. Considering the flatness, stiffness, and effective contact area of wafers and spacer, the thickness difference between top and bottom has controlled to ensure the precise of sample. In the experiment, a backward wave oscillator (BWO) made by MicroTech Instruments was used as the THz emitter to investigate the transmission properties of sample. The detailed experimental setup has been described in Ref. 7.

After post-processing, the transmission curve for normal incidence measured in experiment is illustrated in Fig. 3 with the blue line. For comparison, the calculated result by TMM and simulated one by COMSOL Multiphysics® with "*RF Module/In-Plane Waves*" are both illustrated in Fig. 3 with the red and green lines, respectively. The experimental results show that the sample we designed is a THz filter with high transmissivities (~70%), triple quasi-equidistant channels (~14 GHz), narrow peaks (~3 GHz), and high quality (~100 ×). Experimental results agree with theoretical and simulated ones.

In order to reveal more detailed information of the formation of three transmission peaks observed in all of three

TABLE I. A part of calculated evaluation function F values by using Eq. (1) of different cavities thicknesses in configuration SASRSRSAS.

		Thickness of cavity R (mm)			
Value of F		0.92	0.93	0.94	0.95
Thickness of cavity A (mm)	1.03	255.6	259.8	260.5	255.2
	1.04	245.9	254.7	260.7	258.8
	1.05	231.0	244.0	254.1	260.2
	1.06	215.5	232.6	243.3	252.4

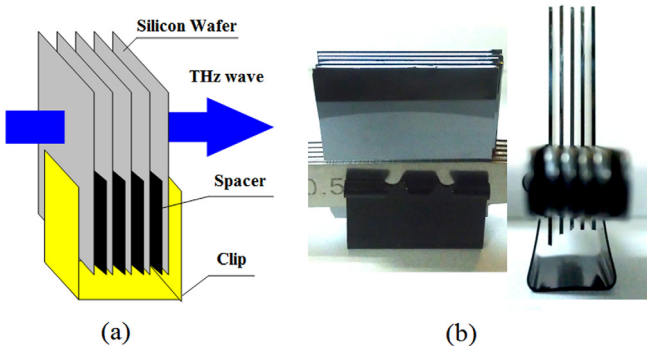

FIG. 2. The structure of the sample: (a) schematic drawing and (b) photograph.

methods, we performed the electronic field distribution simulation of three transmission peaks by using COMSOL Multiphysics®, as illustrated in Fig. 4. Obviously, the most energy gathers in the two 1.04 mm-thick air layers in Fig. 4(b), which indicates that the lowest frequency peak is formed by the superposing of two thick cavities in the sides. In contrast, Figs. 4(c) and 4(d) show the most energy gathers in the two 0.94 mm-thick air layers. Furthermore, the two higher transmission peaks are formed by the coupling of two thin cavities in the middle but one is asymmetric and the other is symmetric.

This phenomenon can be explained by the theory of resonant mode coupling, which has been applied widely in the fields of waveguide and metamaterial.[17–20] In the theory, the whole sample can be treated as a Fabry-Perot resonator. As shown in Fig. 5, the configuration of this structure can be divided into four single-cavity resonant systems. Two of them are SAS, and others are SRS. The central frequencies of transmission peaks for each single-cavity system can be decided by considering the FPR effect.[8] By calculation with TMM, the central frequencies of two type single-cavity system (SAS & SRS) are 289.38 GHz and 304.08 GHz. The two eigenmodes of single-cavity resonant system are denoted as $|\omega_1\rangle$ and $|\omega_2\rangle$ in Dirac notation system. However, in our

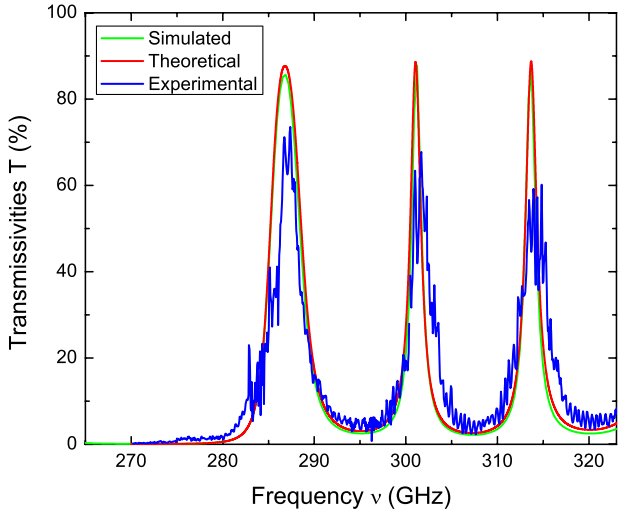

FIG. 3. The transmission curves at normal incidence obtained via different ways: Simulated results by COMSOL (green line); theoretical results by TMM (red line); experimental results by BWO system (blue line).

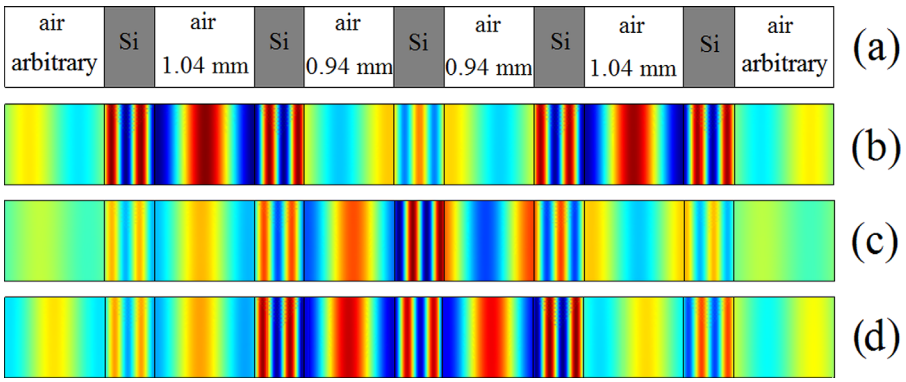

FIG. 4. (a) Structure and thicknesses of layers in simulation. All of Si layers are 525 μm-thick. (b)-(d) The electric field strength distribution of (b) lowest frequency peak; (c) middle frequency peak; (d) highest frequency peak.

experiment, because of their close positions, the two thin cavities in the middle can act as a coupling tunnel between the two thick cavities. There are two kinds of the coupling methods for the middle cavities: Symmetrically and asymmetrically, which should make the eigenmode $|\omega_2\rangle$ split into two new modes (denoted as $|\omega_-\rangle'$ and $|\omega_+\rangle'$). Besides, the two thick cavities on the side can simply superpose by each other (new mode denoted as $|\omega_0\rangle'$). Considering the energy of asymmetric coupling modes is lower than symmetric ones intrinsically and the energy of $|\omega_1\rangle$ is lower than $|\omega_2\rangle$ because of its larger cavity thickness, the peaks whose central frequencies are 286.80 GHz, 301.06 GHz, and 313.68 GHz in theoretical calculation are corresponding to $|\omega_0\rangle'$, $|\omega_-\rangle'$, and $|\omega_+\rangle'$, respectively (the relative energy levels of all modes mentioned are shown as the vertical position in Fig. 5).

In addition, the central frequencies of $|\omega_-\rangle'$ (301.06 GHz) and $|\omega_+\rangle'$ (313.68 GHz) are not symmetrical to the one of eigenmode $|\omega_2\rangle$ (304.08 GHz.). We calculated the central frequencies of transmission peaks of four typical sub-structures in our sample: SAS, SRS, SRSRS, and SASRSRSAS, as listed in Table II. We find both processes of mode splitting from SAS to SASAS (red line in Fig. 1) and SRS to SRSRS (caused by the symmetrically and asymmetrically coupling) are symmetrical to the origin eigenmodes. But for the main structure, SASRSRSAS, the central frequencies of these two splitted new modes are not symmetrical to the one of $|\omega_2\rangle$. The reason is that the central frequencies of $|\omega_+\rangle'$ and $|\omega_-\rangle'$ in SASRSRSAS are not equal to the ones of $|\omega_+\rangle$ and $|\omega_-\rangle$ in SRSRS, respectively. Comparing the configuration of SRSRS and SASRSRAS, the only difference is whether the outside thickness air cavities exist. The mismatch between theory and our previous analysis is caused by interaction between the thin and thick resonance cavities.

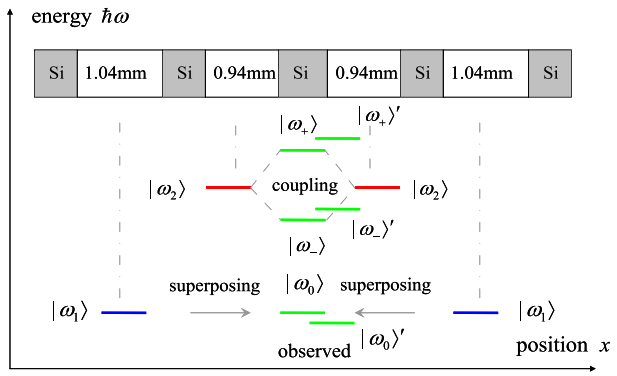

FIG. 5. The analysis chart of modes formation. Blue bars: The eigenmodes of SAS. Red bars: the eigenmodes of SRS. Green bars: The produced modes by coupling and superposing and modified ones considering the interaction between each other. Grey lines: Process of formation.

The mechanism of the shift of the central frequencies in main structure SASRSRSAS is clear. The eigenmode $|\omega_2\rangle$ (for SRS) splits into two modes, $|\omega_-\rangle$ and $|\omega_+\rangle$ (for SRSRS) by symmetrically and asymmetrical coupling. Adding two additional thick cavities on the side (SASRSRSAS) will generate three splitted modes: the lower resonant mode $|\omega_0\rangle'$ comes from the eigenmode $|\omega_1\rangle$ (for SAS); the two higher resonant modes $|\omega_-\rangle'$ and $|\omega_+\rangle'$ come from $|\omega_-\rangle$ and $|\omega_+\rangle$ (for SRSRS). The interaction between the thin and thick resonant cavities makes the central frequencies shift ($|\omega_1\rangle$ to $|\omega_0\rangle'$, $|\omega_-\rangle$ to $|\omega_-\rangle'$, and $|\omega_+\rangle$ to $|\omega_+\rangle'$, as shown in Fig. 5), which indeed generate three transmission observed in all of experiment, calculation, and simulation (blue line in Fig. 1).

Besides, we also measure the effect of oblique incidence on transmission properties. The transmission curves of different incident angle are shown in Fig. 6. In the situation of 15°, the outline still remains as the one of normal incidence. The blue shifts of resonant peaks attribute to the change of effective refractive indices.[12] In the situation of 30°, the heights of peaks greatly reduce and rising of transmission valleys are also clearly illustrated. The borderlines of transmission peaks are hard to distinguish, especially for peak of the highest frequency.

In conclusion, we used silicon and air to fabricate a multi-cavity resonant system with three high quality transmission peaks and applied BWO to perform the transmission properties of THz wave in frequency domain. The sample has advantage as low cost and easy fabricated and is of importance to realize the THz-WDM. From the experimental results, the filter phenomenon is observed and the transmission curves are obtained. There are three high quality

TABLE II. The central frequencies (GHz) of modes in different configuration.

Configuration	Modes and their frequencies		
SAS	$\|\omega_1\rangle$:289.38	–	–
SRS	–	$\|\omega_2\rangle$:304.08	–
SRSRS	–	$\|\omega_-\rangle$:297.53	$\|\omega_+\rangle$:310.63
SASRSRSAS	$\|\omega_0\rangle'$: 286.80	$\|\omega_-\rangle'$: 301.06	$\|\omega_+\rangle'$:313.68

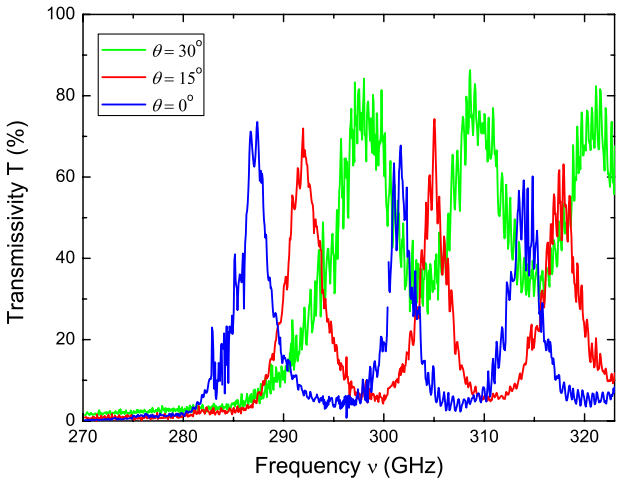

FIG. 6. Transmission curves for different incident angles obtained in BWO system.

transmission peaks which are formed by the coupling of two middle thin cavities. Besides, the side thick cavities also affect the position of transmission peaks. The blue shifts depended on incident angle are also observed in experiment.

We convey thanks to Professor Zhi Hong from Terahertz Science & Technology Laboratory, Zhejiang Institute of Metrology for their kindness and help in the experiment measuring. This work was partly supported by the Shanghai Basic Research Program (11ZR1425000), the Major National Development Project of Scientific Instrument and Equipment (2011YQ150021), the Key Scientific and Technological Project of Shanghai Municipality (11DZ1110800) (12142200100), National Natural Science Foundation of China (11174207) (61138001) (61007059) (61205094), and the Leading Academic Discipline Project of Shanghai Municipal Government (S30502).

[1]B. Ferguson and X. C. Zhang, Nature Mater. **1**, 26 (2002).
[2]P. H. Siegel, IEEE Trans. Microwave Theory Tech. **50**(3), 910–928 (2002).
[3]J. Xu, L. Chen, L. Xie, S. Du, M. Yuan, Y. Peng, and Y. Zhu, Plasmonics **8**, 1293–1297(2013).
[4]S. Biber, A. Hofmann, R. Shulz, M. Collischon, and J. Weinzierl, IEEE Trans. Microwave Theory Tech. **52**(9), 2183–2189 (2004).
[5]D. Wu, N. Fang, C. Sun, X. Zhang, W. J. Padilla, D. N. Basov, D. R. Smith, and S. Schultz, Appl. Phys. Lett. **83**(1), 201–203 (2003).
[6]I. H. Libon, S. Baumgartner, M. Hempel, N. E. Hecker, J. Feldmann, M. Koch, and P. Dawson, Appl. Phys. Lett. **76**(20), 2821–2823 (2000).
[7]J. He, P. Liu, Y. He, and Z. Hong, Appl. Opt. **51**(6), 776–779 (2012).
[8]W. Shen, X. Sun, Y. Zhang, Z. Luo, X. Liu, and P. Gu, Opt. Commun. **282**, 242–246. (2009).
[9]C. J. Wu and Z. H. Wang, Prog. Electromagn. Res. **103**, 169–184 (2010).
[10]W. Withayachumnankul, B. M. Fischer, and D. Abbott, Opt. Commun. **281**, 2374–2379 (2008).
[11]X. Dai, Y. J. Xiang, S. C. Wen, and H. Y. He, J. Appl. Phys. **109**, 053104 (2011).
[12]H. C. Hung, C. J. Wu, and S. J. Chang, J. Appl. Phys. **110**, 093110 (2011).
[13]J. S. Li, Opt. Commun. **283**, 2647–2650 (2010).
[14]J. A. Zhu, L. Chen, J. M. Xu, S. J. Li, and Y. M. Zhu, Opt. Commun. **284**, 5130–5134 (2011).
[15]L. Chen, Z. Q. Cao, F. Ou, H. G. Li, Q. S. Shen, and H. C. Qiao, Opt. Lett. **32**, 1432–1434 (2007).
[16]L. Chen, X. B. Liu, Z. Q. Cao, and S. L. Zhuang, J. Opt. **13**, 035002 (2011).
[17]H. Guo, N. Liu, L. Fu, T. P. Meyrath, T. Zentgraf, H. Schweizer, and H. Giessen, Opt. Express **15**, 12095–12101 (2007).
[18]K. Aydin, I. M. Pryce, and H. A. Atwater, Opt. Express **18**(13), 13407–13417 (2010).
[19]L. Chen, C. Gao, J. Xu, X. Zang, B. Cai, and Y. Zhu, Opt. Lett. **38**, 1379–1381 (2013).
[20]L. Chen, Y. M. Zhu, X. F. Zang, B. Cai, Z. Li, L. Xie, and S. L. Zhuang, "Mode splitting transmission effect of surface wave excitation through a metal hole array," Light Sci. Appl. **2**, e60 (2013).